Original Research

Low serum mesothelin in pancreatic cancer patients results from retention of shed mesothelin in the tumor microenvironment

Xianyu Zhang [a], Yunkai Yu [b], Cody J. Peer [c], Rebekah Landsman [a,1], Nebojsa Skorupan [a,d], Liang Cao [b], Christine Alewine [a,*]

[a] Laboratory of Molecular Biology, Center for Cancer Research, National Cancer Institute, National Institutes of Health, Besthesda, MD, 20892-4264, USA
[b] Genetics Branch, Center for Cancer Research, National Cancer Institute, National Institutes of Health, Besthesda, MD, 20892-4264, USA
[c] Clinical Pharmacology Program, Center for Cancer Research, National Cancer Institute, National Institutes of Health, Besthesda, MD, 20892-4264, USA
[d] Medical Oncology Program, Center for Cancer Research, National Cancer Institute, National Institutes of Health, Bethesda, MD, 20892-4264, USA

A R T I C L E   I N F O

A B S T R A C T

Mesothelin (MSLN) is overexpressed by many cancers, including pancreatic ductal adenocarcinoma (PDAC) and has consequently become a target for anti-cancer therapeutics. Mature, membrane bound MSLN is cleaved by proteases, releasing a shed form that transits to the circulation. Many patients with mesothelioma and ovarian cancer have abnormally high serum MSLN concentration. However, serum MSLN concentration in PDAC patients rarely exceeds levels of healthy controls. Here, serum MSLN concentration in advanced PDAC patients was examined pre- and post-treatment. Serum MSLN did not correlate with tumor MSLN expression, nor with changes in tumor burden as assessed by PDAC serum tumor marker CA19–9. Subsequently, tumor-bearing mouse models were used to investigate the fate of shed MSLN in PDAC versus a control cervical cancer model. Efficiency of MSLN secretion into the serum was cell-line dependent. Tumors from some PDAC lines had poor MSLN secretion efficiency although these lines had similar or higher MSLN shedding rate, total and surface MSLN expression. Measurements of compartment-specific MSLN concentration taken at equilibrium suggested that tumors with poor MSLN secretion efficiency trapped shed MSLN in the tumor microenvironment (TME), a finding confirmed by dynamic experiments using a doxycycline-inducible MSLN expression system. Tumors with the poorest MSLN secretion efficiency had higher collagen density and increased abundance of MSLN binding partner MUC16. The tumor with the worst secretion efficiency could rebind shed MSLN to the cancer cell surface. Altogether, these data suggest that PDAC can trap shed MSLN within the TME. This finding has potential significance for design of MSLN-targeted therapeutics.

Introduction

Mesothelin (MSLN) is a surface protein primarily expressed by mesothelial cells forming the pleura, pericardium and peritoneum [1]. The *MSLN* gene encodes a 70 kD precursor protein which is cleaved by intracellular proteases [2], to produce single molecules of mature 40 kD MSLN and a second, secreted protein called Megakaryocyte Potentiating Factor (MPF). Mature MSLN undergoes glycophosphoinositol (GPI) modification permitting linkage to cell membranes and is detectable on the cell surface [3]. Mature, membrane-bound MSLN can be cleaved

near the C-terminus by the action of surface proteases resulting in shedding of soluble [4,5]. Soluble MSLN transits to the circulation and can be detected at low levels in healthy volunteers [6]. Factors which control the transit of MSLN from cell surface to serum have never been investigated.

Many solid tumors overexpress MSLN, and higher expression has been linked to poorer prognosis in numerous tumor types [7]. Mesothelioma, epithelial ovarian cancer and pancreatic ductal adenocarcinoma (PDAC) have some of the highest incidences of tumor MSLN expression [8,9]. Estimates suggest that >70% of these tumors express

MSLN. Serum MSLN is also elevated in many patients with MSLN-expressing mesothelioma and ovarian cancer [10]. Although testing for elevated serum MSLN is neither sensitive nor specific enough for use as a cancer diagnostic, serial measurements of serum MSLN can be used to follow tumor growth trajectory in mesothelioma patients [11, 12]. By contrast, elevated serum MSLN is not typically observed in patients with MSLN-expressing PDAC [13]. Here, we have explored this observation in both patients and mouse models of PDAC with the aim of better understanding the fate of shed MSLN in PDAC.

Materials and methods

Collection of patient samples

Blood samples from PDAC patients with previously treated advanced disease were collected between August 2016 and June 2019 on Institutional Review Board-approved protocol NCT02810418 at the NIH Clinical Center (Bethesda, MD). Informed consent was obtained from all participants. Patient treatment and demographic data are described in [14].

Assay of serum MPF and MSLN

MSLN concentrations reported for the experiments in Fig. 2 were determined using DMSLNO Kit (R&D Systems) as per manufacturer's instructions. For all other experiments, electrochemiluminescence immunoassay was used to determine the MSLN and MPF concentrations. MPF was assayed as described previously [11,12] and in Supplemental Methods.

Cell culture and reagents

Human PDAC cell lines (KLM1, T3M4) and KB cervical cancer cell line (a HeLa derivative) were the gifts of Udo Rudloff, Mitchell Ho, and Ira Pastan (all of NCI, Bethesda, MD), respectively. AsPC1 was purchased from ATCC. Identity of the cell lines was confirmed by STR testing. Meso16 and Meso29 patient-derived primary cell lines were provided by Raffit Hassan (NCI, Bethesda, MD) and have been previously described [15]. Cells were cultured as described in Supplemental Methods. Doxycycline hyclate (CAS 24,390–13–5, EMD) was dissolved in 0.9% NaCl to 50 mg/ml. Stock solution was diluted to 500 μg/ mL with PBS then sterile filtered (0.2 μM). Doxycycline chow (200 mg/ kg; S3888) was purchased from Bio-Serv.

Engineering MSLN knock-out (KO) cell lines

CRISPR-Cas9 gene editing was utilized to KO *MSLN* gene expression from KLM1, T3M4 and KB cell lines. KLM1 MSLN KO cells were previously characterized [16]. KB and T3M4 MSLN KO cell lines were generated by using IDT Alt-R CRISPR-Cas9 System as per the manufacture's instruction and detailed in Supplemental Methods. Alt-R® CRISPR-Cas9 crRNA: Hs.Cas9.MSLN.1.AA (Supplemental Figure 1A) was purchased from IDT Technologies to target exon 3 of MSLN variant 1. Clonal lines lacking MSLN expression were established by fluorescence-activated single cell sorting (FACS) gated on MSLN expression. MSLN gene alteration was confirmed by Alt-R® Genome Editing Detection Kit (IDT 1,075,932). Validation of MSLN KO was demonstrated by flow cytometry (See Supplemental Figure 1B-C).

Engineering cell lines with inducible MSLN expression

Inducible pLVX-TetOne-Puro-MSLN lentiviral vector was engineered by adding the hMSLN ORF into TAKARA pLVX-TetOne-Puro Vector backbone. The plasmid was packed into lentivirus by NINDS Viral Production Core (Bethesda, MD). Each MSLN KO cell line (KB, KLM1, T3M4) was transduced with the lentivirus, and selected in puromycin (1 μg/ml). Cells were treated with dox (1 μg/ml) to induce MSLN expression and the MSLN(+) population was identified and collected by FACS.

Mouse experiments

All animal experiments were performed in accordance with NIH guidelines and approved by the NCI Animal Care and Use Committee. Female 6–8 week-old athymic nude mice (Charles River, Frederick, MD) were inoculated subcutaneously with 3×10^6 cells in 4.0 mg/mL Matrigel (Corning, NY) in RPMI 1640 (Gibco, MD) with no additives. Tumor size was measured in two dimensions by digital calipers and tumor volume was calculated using the formula: 0.4 x width^2 x length.

Intratumoral fluid (ITF) preparation

Harvested tumors were suspended in 750 μl of RPMI 1640 (Gibco, MD) with no additives. Tumor was cut into fine pieces using surgical scissors, re-suspended in an additional 750 μl of RPMI, and tumor debris spun down at 200x*g* for 3 min at 4 °C. Supernatant was recovered and frozen at −80 °C in aliquots until analysis.

Histological analyses

Tumor samples were sent to the NCI Pathology/ Histotechnology Laboratory core facility for all histologic analyses.

Mathematical modeling of MSLN transit

A semi-mechanistic model was built to describe the kinetics of MSLN generation, maturation, shedding, and degradation in pancreatic versus non-pancreatic tumor types (Phoenix NLME, Certara, Princeton, NJ) as described in Supplemental Methods and Supplemental Figure 2.

Statistics

Data are presented as averages with error bars representing standard deviations unless stated otherwise. Statistical significance is indicated as follows: ns = not significant, * for $p < 0.05$, ** for $p < 0.01$, *** for $p < 0.001$. All experiments were confirmed by repeat.

Results

Serum MPF and MSLN remain within normal range throughout treatment

MSLN and MPF expression in serum were assessed in a cohort of PDAC patients who had not received systemic therapy for ≥ 2 weeks. Mean serum MSLN (mean: 0.856 nM, range: 0.291- 1.54 nM) and MPF (mean: 0.511 ng/mL, range: 0.150–1.61 ng/mL) concentrations in this population (Fig. 1A) tested within the range previously reported for healthy donors [6], less than 1.5 nM for MSLN [17], and less than 1.2 ng/mL for MPF [11]. A moderately strong positive correlation between serum MSLN and serum MPF was observed, consistent with the two proteins' evolution from a single protein precursor molecule (Fig. 1B). Archival tumor samples were available for immunohistochemistry analysis in 18 of 38 patients with pancreatobiliary cancer. All 18 patients had detectable MSLN expression in their archival tumor tissue, however, more robust tumor MSLN expression did not correlate with increased serum MSLN concentration (Fig. 1C). This data confirms previous reports that patients with advanced PDAC most often do not have increased serum MSLN or MPF despite expression of MSLN in tumor tissue.

Since MSLN shed by tumor cells and normal mesothelium is the source of serum MSLN, we predicted that serum MSLN should act as a tumor marker and fluctuate with tumor growth or regression. Therefore, we compared change in serum MSLN concentration before and after treatment for any association with change in CA 19–9, the most utilized
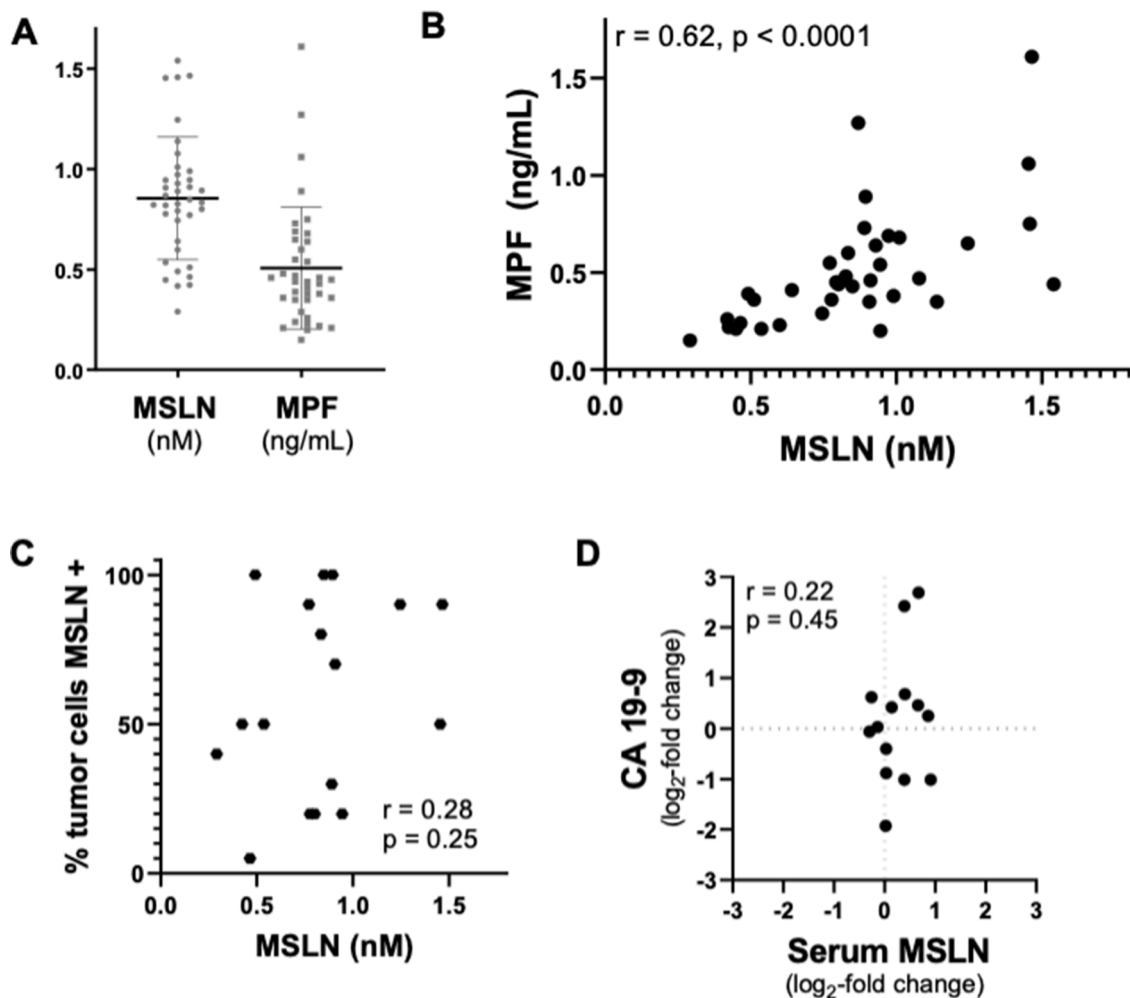
Fig. 1. A) Baseline serum MSLN and MPF in PDAC patients treated on Phase I/II study of mesothelin-targeted immunotoxin LMB-100 with or without nab-paclitaxel. B) Correlation between serum MSLN and serum MPF at baseline. C) Relationship between cancer cell expression of MSLN in archival tissue samples versus serum MSLN at baseline. D) Relationship between change in serum MSLN with treatment to change in bona fide PDAC tumor marker CA 19–9. Only patients with detectable CA 19–9 that trended with disease burden were considered evaluable for this analysis.

blood tumor marker for approximating tumor growth trajectory in patients with PDAC. Fig. 1D shows fold-change in CA 19–9 vs serum MSLN between pre-treatment and end of study measurements in patients with evaluable CA19–9. No correlation was observed in the 13 evaluable samples, suggesting that serum MSLN is unlikely to trend with tumor burden. Taken together, these data suggest that tumor shed MSLN makes little to no contribution to serum MSLN levels in PDAC patients.

MSLN secretion efficiency is a cell-line dependent property

To determine why MSLN-expressing PDAC fails to secrete enough soluble MSLN to raise serum MSLN levels above the normal range, we modeled the process in mice. KLM1, T3M4 and AsPC1 human PDAC cell lines, all of which strongly express MSLN, were grown subcutaneously in nude mice until tumors reached at least 100 mm^3 then serum samples were obtained. The MSLN-expressing cervical cancer cell line KB, previously shown to robustly secrete MSLN into mouse serum [18], was used as a positive control. Since our ELISA assay for serum MSLN does not recognize the murine isoform of MSLN, MSLN is not detectable in the serum of tumor-naïve mice. We observed that serum MSLN concentration rose as tumor size increased, although the rate of rise varied by cell line (Fig. 2A). Replotting these data to show serum MSLN concentration per gram of tumor, an estimation of MSLN serum secretion efficiency, the values cluster around a unique constant for each cell line (Fig. 2B).

KB and AsPC1 had the highest secretion efficiency. T3M4 secretion efficiency was significantly less, and KLM1 secreted the least serum MSLN per gram of tumor. These data demonstrate that the KLM1 and T3M4 cell lines have low serum MSLN secretion efficiency and could model the low/ non-secretor phenotype observed in patients with PDAC.

One possible explanation for the less efficient secretion of MSLN into the serum of KLM1- and T3M4-bearing mice is that these cells have lower surface expression of MSLN and therefore less MSLN available for shedding than KB or AsPC1. However, assessment of MSLN surface expression using flow cytometry showed that KLM1 has much higher MSLN surface expression than KB, while T3M4 surface MSLN expression is only slightly higher than KB (Fig. 2C). Possibly, KB cells might shed MSLN more rapidly than the two PDAC lines, resulting in more efficient MSLN secretion. To assess this, we measured shedding rates of the cell lines in culture. While the Meso29 mesothelioma control cell line was found to shed MSLN approximately twice as fast as KB cells, there was no statistically significant difference in the shedding rates of T3M4 or KLM1 compared to KB, although KLM1 shedding trended slower and T3M4 faster (Fig. 2D). These data demonstrate that serum MSLN levels for KB tumors are unlikely to be higher due to increased shedding by these cells, especially as compared to T3M4. Instead, they suggest that another intrinsic property of T3M4 and KLM1 tumors prevents efficient secretion of MSLN into serum.
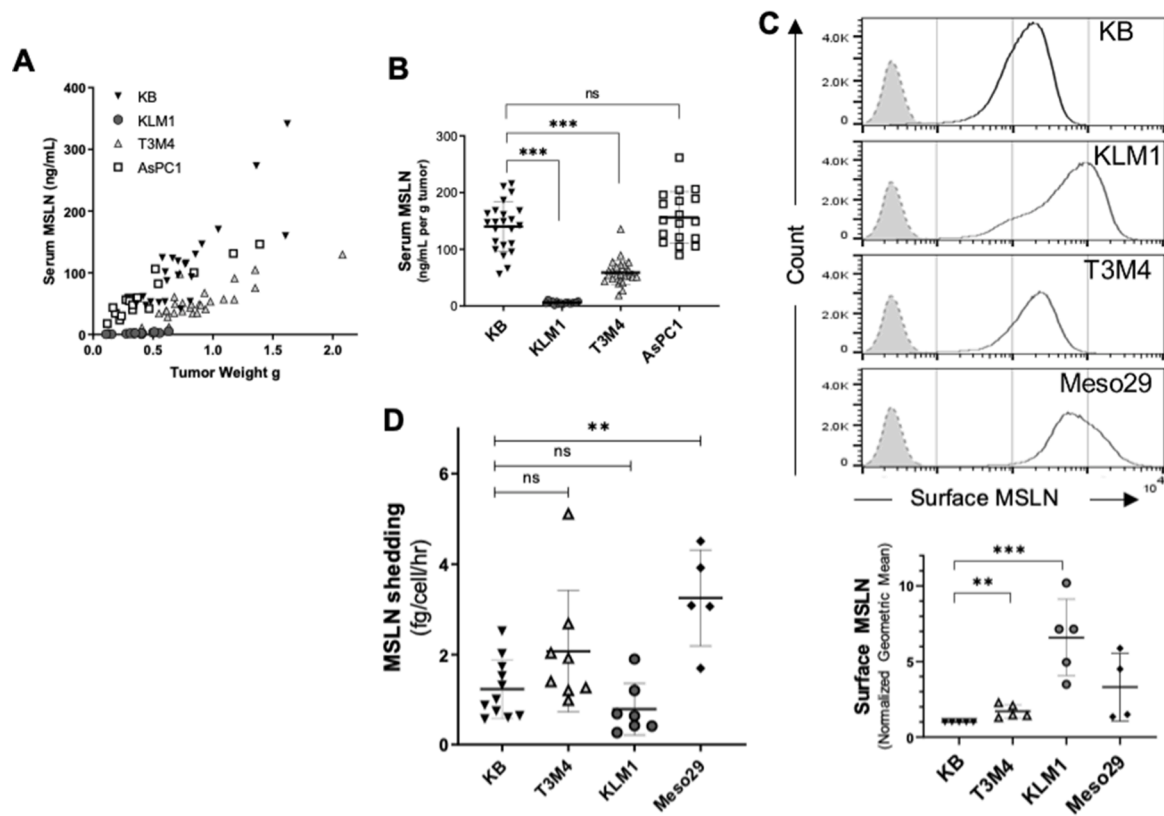
Fig. 2. Efficiency of MSLN secretion into serum is characteristic of cell type. A & B) Concentration of hMSLN in the serum of athymic nude mice bearing subcutaneous tumors was analyzed by ELISA. A) For each mouse in four independent experiments, serum MSLN concentration was plotted versus tumor weight. Slope [95% CI] expressed in ng/mL serum MSLN per g tumor: KB 181 [128–233], KLM1 6.75 [3.80–9.71], T3M4 65.3 [45.5–85.1], AsPC1 97.0 [76.1–118] B) Secretion efficiency of MSLN, defined as serum MSLN per tumor weight, is a constant value the four cell types tested. C) Flow cytometry tracings showing surface MSLN on the indicated cell types. Representative image from at least 3 runs is shown. Graph below compares geometric means of surface MSLN expression normalized to value for KB for each experiment. Meso29 is a mesothelioma cell line used as a positive control. D) MSLN shedding rate was calculated by serial ELISA measurements of MSLN concentration over 6 h in a known volume of medium for a set number of cells.

*Steady state MSLN and MPF concentrations in tumor compartments*

To better understand how MSLN localizes within tumors, we assayed MSLN and MPF concentrations by ELISA in the ITF fraction, the post-extraction tumor remnant lysate, total (unextracted) tumor lysate and serum (Fig. 3A). Lower MSLN concentration was found in the ITF and serum fractions of KLM1 and T3M4 as compared to KB (Fig. 3B), despite similar amounts of MSLN in total tumor lysate and remnant lysate (Fig. 3C). These data demonstrate that a barrier must exist during transit of MSLN from tumor cells to the ITF. This could occur due to decreased shedding of MSLN from T3M4 and KLM1 tumor cells in vivo, however, these tumor cells had similar shedding rates when measured in vitro (Fig. 2D). Alternatively, shed MSLN in T3M4 and KLM1 tumors may be trapped within the tumor remnant. If trapping is occurring, this should inflate the concentration of MSLN observed at steady state in T3M4 and KLM1 tumors. In ITF, mean MSLN concentration for KB was >3-fold higher than KLM1 and >2-fold higher than T3M4 (8.50×10^2, 2.51×10^2, and 3.70×10^2 ng per g of tumor, respectively). In serum, the gap between mean MSLN concentration for mice bearing KB tumors and the pancreatic tumors was much higher: >50-fold higher as compared to KLM1 and ~3.5-fold higher than T3M4 (2.73×10^2, 5.41, and 7.80×10^1 ng/mL per g of tumor, respectively). These data are consistent with the presence of a second barrier which impairs transit of MSLN between ITF and serum, particularly in KLM1 tumors.

To clarify the mechanisms responsible for these barriers, MPF concentrations were measured in the same samples. MPF is synthesized at a 1:1 ratio to MSLN but does not require sheddase activity for release from tumor cells, eliminating one variable from the model system. We found

that serum MPF concentration was highest in KB, followed by T3M4, and lowest in KLM1 (Fig. 3D), just as seen for serum MSLN (Fig. 3B). However, KLM1 had much lower total tumor MPF concentration compared to KB and T3M4 (Fig. 3E), suggesting that less MPF (and therefore MSLN) is made by KLM1 tumors. Similar concentrations of MPF were found in KLM1 ITF as compared to KB ITF despite much lower serum MPF concentration in KLM1, suggesting that a second barrier exists in KLM1 tumors which reduces efficiency of MPF transport from ITF to serum, causing accumulation of MPF in ITF. For T3M4, MPF concentration was similar to KB in total tumor specimens (Fig. 3E). KB and T3M4 tumors also had similar concentrations of MPF in ITF, even though T3M4 had much lower ITF MSLN concentration than KB. Despite this, serum MPF concentration was much lower in mice bearing T3M4 tumors than those with KB tumors (Fig. 3D), consistent with the existence of a barrier preventing transit of MPF from ITF to serum in T3M4, too. Further, MPF in T3M4 tumor remnant was much higher compared to KB, implying that secretion of MPF from T3M4 cells could be slower than secretion from KB cells. Alternatively, our ITF extraction process may have been less efficient in T3M4 than in KB. In summary, these data support that both KLM1 and T3M4 tumors have a barrier that reduces both MPF and MSLN transit between ITF and serum. This barrier appears to be independent of reduced MSLN expression or shedding rate which could also contribute to reduced serum MSLN concentrations in the PDAC models.

Determining the rate of MSLN transit between compartments

We engineered genetically modified variants of the KB, KLM1 and T3M4 cell lines to assess MSLN transit. CRISPR-Cas9 gene editing was
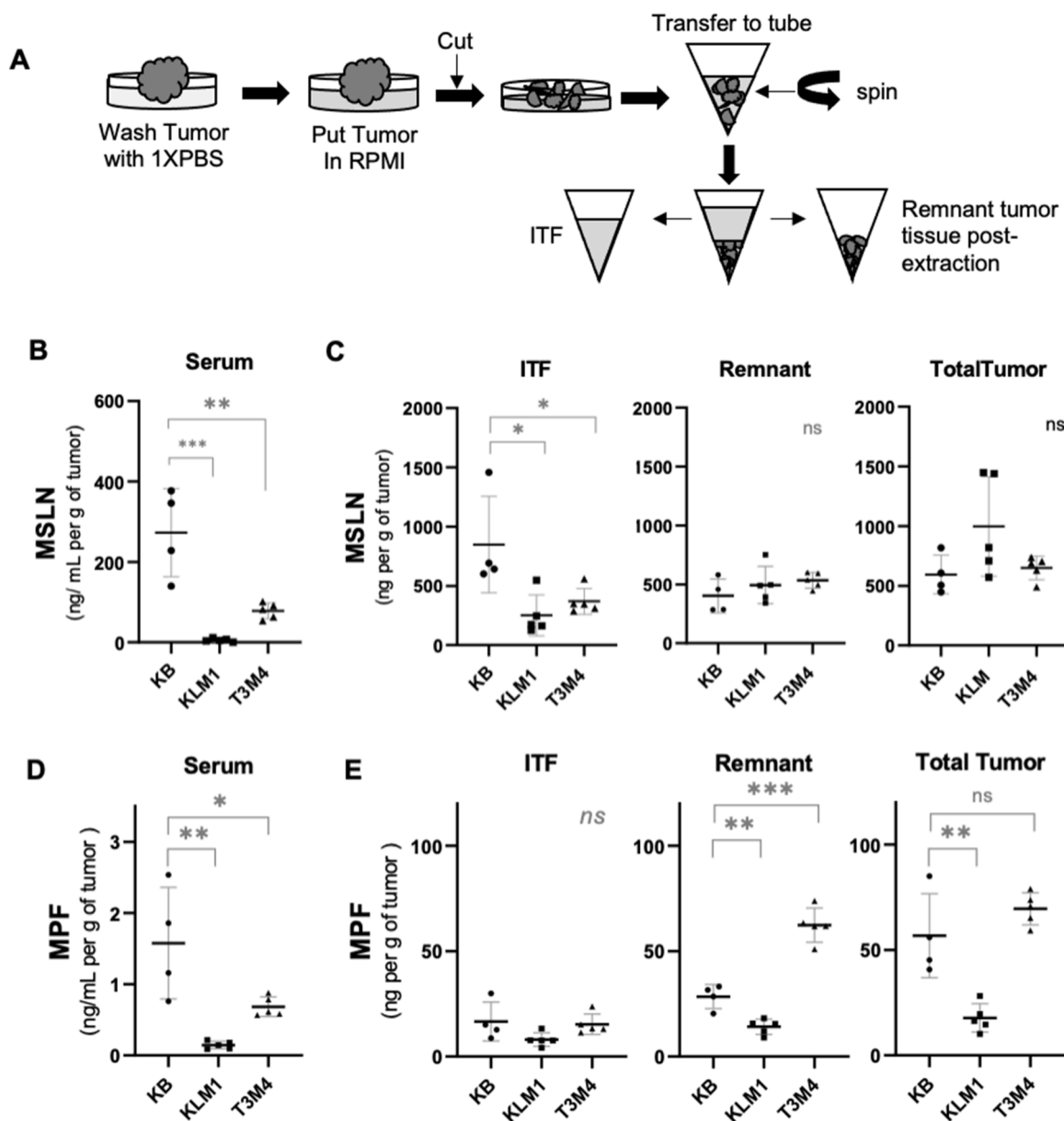
Fig. 3. Compartment-specific measurements of soluble MSLN and MPF at steady state. Nude mice were inoculated subcutaneously with the indicated cell types and tumors were permitted to grow to size >100 mm³. Harvested tumors were processed as shown in (A). ITF = intratumoral fluid. ITF was isolated from a known mass of tumor by resuspending freshly harvested tumors in equivolume, unsupplemented (serum-free) tissue culture medium, finely mincing tumor, and removing the remaining tumor debris by centrifugation.
Measurements of soluble MSLN (B-C) and MPF (D-E) in serum, ITF, total tumor lysate, and lysate from remnant tumor following ITF extraction as measured by ELISA are shown.

used to disrupt the native *MSLN* locus and then KO lines were transduced with a plasmid containing a doxycycline(dox)-inducible MSLN expression cassette. Exposure of the resulting KB+, KLM1+ and T3M4+ cells lines to dox initiated MSLN expression, although these cell lines expressed no detectable MSLN in the absence of dox (Fig. 4A). Mice bearing mature, subcutaneous tumors were treated with IP dox (100 μg) and transitioned to dox-containing chow (200 mg/kg ad lib) at time 0 to initiate MSLN production. Tumors and serum were harvested at multiple timepoints and MSLN concentrations were assessed in the 4 compartments described in Fig. 3A. MSLN was detectable in all compartments by 6 h, the earliest post-induction timepoint assessed, and increased at later timepoints up to 36 h (Fig. 4B-D). The rate of this rise slowed for all compartments between 12 and 24 h post-induction, suggesting that MSLN concentrations were approaching steady state levels (4C-D). Use of the dox-inducible exogenous promoter caused overexpression of

MSLN compared to exogenous MSLN production by the parent tumor lines (Fig. 3B & 3C, Fig. 4B; Supplemental Table 1). Despite this, steady state (36-hour timepoint) MSLN concentration was still lowest in KLM1 in every compartment (Fig. 4B). At steady state, mean serum MSLN was nearly a log-fold lower for KLM1+ than for T3M4+ (7.76×10^2 ng/mL per g of tumor [$\pm 5.92 \times 10^2$ S.D.] versus 4.42×10^3 [$\pm 2.19 \times 10^3$ S.D.]). KB+ serum MSLN was nearly another log-fold higher than that measured for T3M4+ (1.47×10^4 ng/mL per g of tumor [$\pm 2.40 \times 10^3$ S.D.]). Using these data, the ratio of serum/ITF MSLN over time was assessed to determine whether a "barrier" exists between these compartments. For T3M4+ and KB+ cells, the two concentrations were approximately equal, resulting in grand means for this ratio of 1.002 and 0.991, respectively. This data is consistent with lower T3M4 serum MSLN concentration occurring due to reduced expression, shedding rate or a barrier to transit upstream of ITF. By contrast, the serum/ITF MSLN
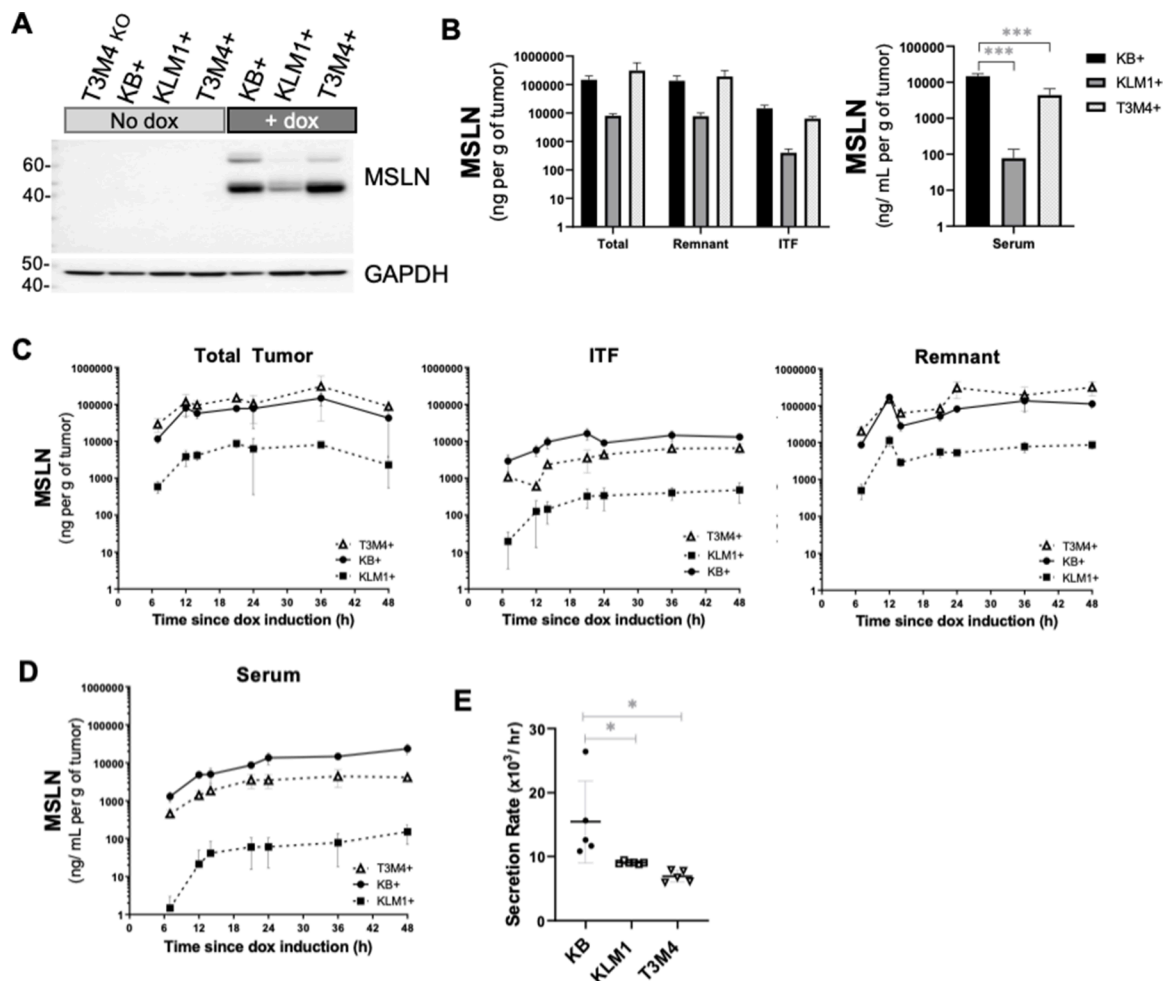
Fig. 4. Measuring transit of MSLN between compartments. A) Immunoblot showing MSLN expression for MSLN knock-out (KO) cell lines transduced with a doxycycline (dox)-inducible MSLN expression plasmid (KB+, KLM1+, T3M4+). GAPDH is loading control. B-E) Nude mice were inoculated subcutaneously with the KB+, KLM1+ or T3M4+ cell lines. Dox treatment was administered by IP drug injection to initiate MSLN expression (time 0) once tumors had reached at least 100mm³, and dox-containing chow was provided ad lib to mice for the remainder of the experiment. Mice (at least 3 for each timepoint) were euthanized at the indicated times and serum, ITF, total tumor and lysate from remnant (RMNT) tumor were assessed by ELISA for MSLN concentration. B) Snapshot of MSLN concentrations at steady state (36 h) for each cell line in each compartment as indicated. C-D) MSLN concentration in indicated compartment as measured over time. E) Rate of MSLN secretion into the serum was calculated using semi-mechanistic modeling as described in Materials and Methods.

ratio in KLM1+ cells was much lower (0.203, ~80% reduction in secretion from ITF to serum relative to T3M4+ and KB+ lines), suggesting that MSLN released into the ITF of KLM1+ cells cannot diffuse into the serum as easily. The rate of MSLN secretion into the serum was also calculated. The two PDAC tumor types had slower secretion than the KB control cell line (Fig. 4E).

Investigation of mechanisms for decreased efficiency of MSLN secretion into serum

PDAC is notorious for the density of the stromal reaction that forms around tumor cells. Trichrome staining of tumors demonstrated increased density of collagen in KLM1 compared to T3M4 and much lower collagen density in KB tumors (Fig. 5A). Given this association between secretion efficiency and collagen density, we hypothesized that MSLN might be trapped in tumors by the stromal matrix and disruption of this matrix might release MSLN. We treated KLM1 tumor-bearing mice with intratumoral trypsin, intratumoral collagenase or heat-inactivated control and compared serum MSLN levels before and after treatment. This maneuver was unsuccessful: treatment with ECM-disrupting enzymes resulted in little to no change in serum MSLN levels (Fig. 5B), although we were unable to measure any change in

matrix provoked by these treatments. We were unable to identify other methods that might disrupt ECM without simultaneously killing tumor cells.

Previous studies have shown that MSLN specifically binds to the cell surface mucin MUC-16 [19]. We hypothesized that increased tumor MUC16 might hold shed MSLN near the tumor, inhibiting serum secretion efficiency. MUC16 expression in each cell line was analyzed by immunoblot. KLM1 had the highest surface MUC16 expression, followed by T3M4, while KB had almost no expression of this MSLN binding partner (Fig. 5C). We considered that shed MSLN could rebind to cancer cells by associating with MUC16, slowing transit to the serum. To assess whether shed MSLN could rebind, KO cells were treated with equi-volume of conditioned medium (CM) containing shed MSLN, then surface MSLN was assessed by flow cytometry. Indeed, exposure of KLM1 KO cells to shed MSLN in CM increased detectable surface MSLN, consistent with rebinding (Fig. 5D). Although T3M4 also expressed significant MUC16 by immunoblot (Fig. 5C), increased surface MSLN was not observed in T3M4 KO cells after CM exposure. While rebinding of shed MSLN may contribute to impaired MSLN secretion efficiency of KLM1, other mechanisms must be responsible for this phenomenon in T3M4.
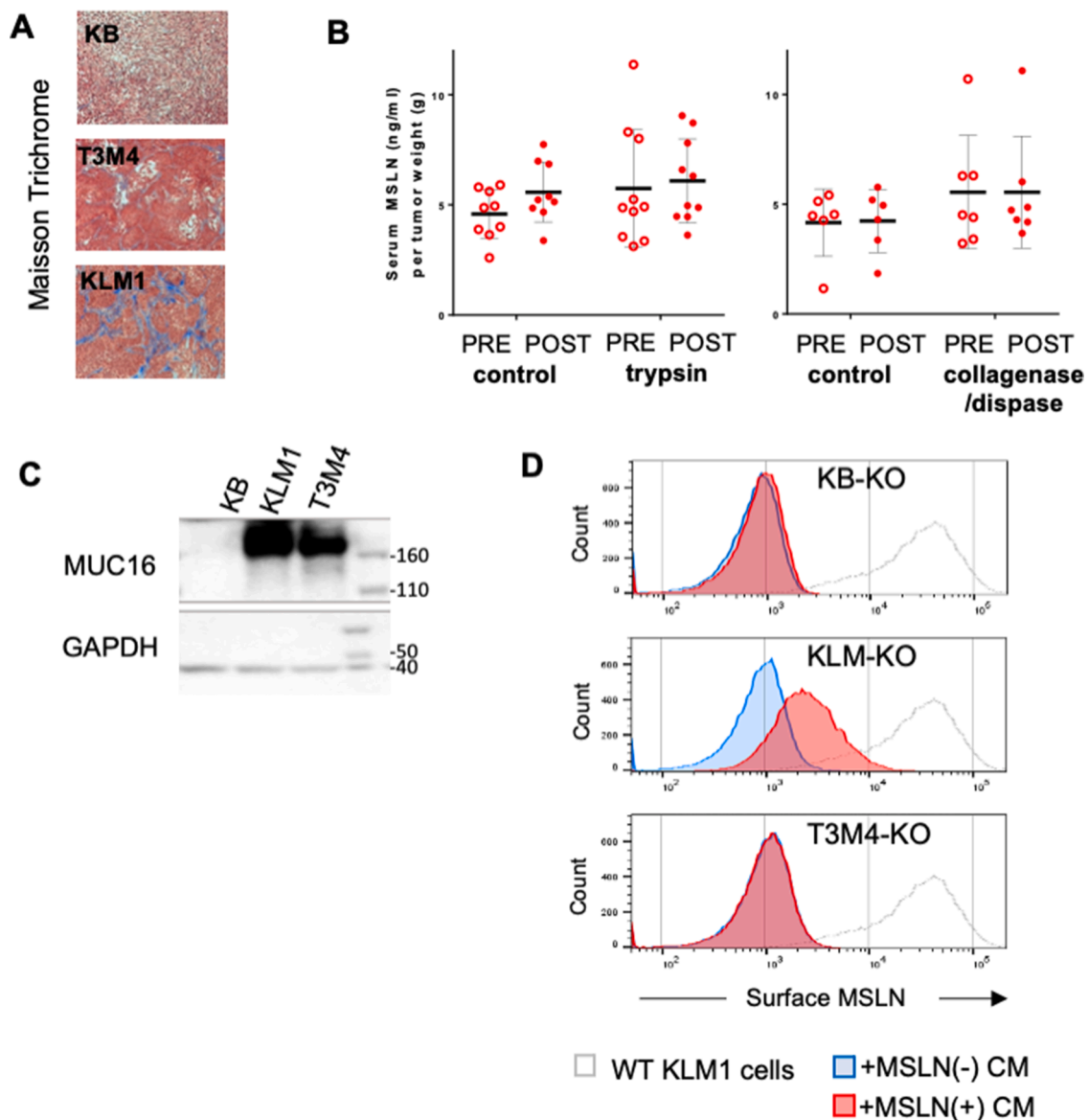
Fig. 5. Low MSLN secretion efficiency is associated with physical properties of tumor. A) Subcutaneous tumors grown in nude mice were stained with Maisson Trichrome to assess collagen density. Representative images are shown. B) Subcutaneous tumors were grown in nude mice as described previously. Once tumors reached ~300mm^3 (left) trypsin or control (trypsin inactivated by boiling for >30 min), or (right) collagen/dispase solution versus control (collagen/dispase inactivated by boiling for >30 min) was injected directly into tumors. Serum MSLN was examined by ELISA pre- and 24 h post-trypsin treatment. C) Immunoblot of tumor lysates showing expression of MSLN binding partner MUC16. GAPDH is used as a loading control. D) Indicated KO cells were incubated with MSLN-containing conditioned medium (red) or control conditioned medium lacking MSLN (blue). Surface MSLN on the KO cells was then measured by flow cytometry. Tracing for MSLN-expressing KLM1 cells is shown as positive control (gray).

Discussion

Despite significant expression of MSLN in PDAC, serum MSLN concentrations in advanced PDAC patients do not exceed those of normal controls. Here, we have also demonstrated that serum MSLN concentrations in advanced PDAC patients do not mirror changes in CA 19–9, an additional piece of evidence that the circulating MSLN concentration does not dependent on cancer cell MSLN production. Our pre-clinical data show for the first time that a barrier exists in the transit of shed MSLN between the TME and serum in two PDAC models. This barrier contributes to lowering the efficiency of tumor secretion of shed MSLN into the serum, leading to accumulation of shed MSLN within the tumor compartment.

Our data raise concern that MSLN shed from cancer cells accumulates within the TME rather than diffusing into the serum. The dynamics of MSLN shedding and serum secretion are predicted to modulate efficacy of some MSLN-targeted therapeutics [20]. For instance, a higher rate of MSLN shedding will reduce opportunities for MSLN-directed therapeutics to interact with membrane-bound MSLN on cancer cells, lowering the efficacy of therapeutics such as antibody-drug conjugates (ADCs) that require cancer cell internalization for anti-tumor activity [21]. When shed MSLN remains trapped within the TME, it could become a decoy receptor and bind MSLN-directed therapeutics before they reach the cell surface, forming a potent site barrier that could limit therapeutic delivery to cancer cells [22]. Conversely, higher concentrations of shed MSLN within the TME might improve efficacy of MSLN-directed tumor diagnostic molecules or therapeutics (such as antibody-radioligand conjugates) that depend only on target accumulation within tumor tissue but do not require direct binding to tumor cells. Although the biology of PDAC presents numerous challenges to

successful development of large molecule therapeutics against any target, our results predict that MSLN-directed therapeutics with anti-tumor activity independent of binding to the cancer cell surface may have improved efficacy compared to those which require direct interaction with MSLN-expressing cancer cells. Alternatively, development of an anti-MSLN antibody that reacts only with GPI-linked MSLN and not with shed MSLN could alleviate this problem. For instance, an ADC which specifically recognizes the residual transmembrane stalk of cleaved amphiregulin, was recently reported [23].

We have demonstrated that tumor secretion efficiency of shed MSLN into serum is cell-line specific. Reduced MSLN expression or shedding rate may play a role in decreased serum MSLN concentrations, but our data have demonstrated that additional factors contribute to MSLN serum secretion efficiency in PDAC tumors. We examined the secretion efficiency both in tumors expressing native MSLN at endogenous levels and also in MSLN KO versions of the same tumor types that overexpress MSLN from a doxycycline-inducible promoter. Despite varying the promoter responsible for driving MSLN expression, impaired serum secretion of MSLN was still observed in the PDAC tumors. While we could not conclusively establish a mechanism for this behavior, we demonstrated negative associations between MSLN secretion efficiency and both tumor collagen density and tumor cell expression of MSLN binding partner MUC16. In KLM1 cells, we also observed that shed MSLN in CM can rebind to the cancer cell surface. While this behavior may be associated with the high levels of MUC16 expressed in KLM1, we were unable to assess this directly in MUC16-deficient cells as the impaired growth caused by reduced/absent MUC16 expression may confound the assay [24]. We hypothesize that rebinding of shed MSLN to KLM1 cells contributes to the especially poor shed MSLN secretion efficiency of KLM1. Overall, the data suggest that multiple factors contribute to the impaired MSLN serum secretion efficiency of PDAC.

Clinical data, including ours, indicate that MSLN secretion efficiency is universally low in PDAC patients, while our cell line data show variable serum secretion efficiency in the three PDAC lines that we tested. Our modeling has several limitations which may account for this discrepancy. First, we grew all tumors subcutaneously to control for tumor localization. It is well understood that TME can differ depending on tumor location. Tumors grown in another location, such as orthotopically in the pancreas, may have additional restrictions on MSLN serum secretion efficiency beyond what we have examined here. In addition, a fully intact immune system (which is not present in our model) could further modulate MSLN serum secretion efficiency. Secondly, we could not investigate whether the efficiency of MSLN secretion changes as tumors grow much larger given the humane endpoints required for ethical use of animals in research. The larger volume of human patients' tumors compared to mouse tumors may impose additional restrictions on MSLN secretion efficiency beyond the scope of our investigation. Further work will be required to delineate additional factors which may contribute to impaired secretion of shed tumor MSLN into serum. Future studies utilizing 3D cell co-culture systems [25] may be advantageous in determining the relative contributions of individual TME components to MSLN trafficking.

In summary, advanced PDAC traps shed MSLN within the TME. Previous studies have shown that intratumoral shed MSLN may act as a decoy receptor to reduce the efficacy of MSLN-targeted anti-cancer therapeutics which require cancer cell surface binding for activity. Trapping of MSLN within pancreatic cancer TME may increase resistance of these tumors to some MSLN-targeted therapeutics.

Funding

Consent

This is not a case report. Patient data reported are lab values. Samples were drawn as part of a treatment study that was performed after obtaining written informed consent from patients.

CRediT authorship contribution statement

Xianyu Zhang: Methodology, Validation, Formal analysis, Investigation, Visualization, Writing – review & editing. **Yunkai Yu:** Methodology, Formal analysis, Investigation, Writing – review & editing. **Cody J. Peer:** Methodology, Software, Formal analysis, Writing – review & editing. **Rebekah Landsman:** Formal analysis, Investigation, Writing – review & editing. **Nebojsa Skorupan:** Data curation, Writing – review & editing. **Liang Cao:** Methodology, Formal analysis, Resources, Supervision, Writing – review & editing. **Christine Alewine:** Conceptualization, Methodology, Formal analysis, Resources, Data curation, Writing – original draft, Visualization, Supervision, Project administration, Writing – review & editing.

Declaration of Competing Interest

None.

Acknowledgments

Supplementary materials

Supplementary material associated with this article can be found, in the online version, at doi:10.1016/j.tranon.2022.101440.

References

[1] K. Chang, I. Pastan, M.C Willingham, Isolation and characterization of a monoclonal antibody, K1, reactive with ovarian cancers and normal mesothelium, Int. J. Cancer 50 (3) (1992) 373–381.

[2] S. Joseph, X. Zhang, L.K. Smith, C. Alewine, Furin is not required for processing of mesothelin precursor protein, Biochim. Biophys. Acta Mol. Cell Res. 1868 (5) (2021) 118967.

[3] K. Chang, L.H. Pai, J.K. Batra, I. Pastan, M.C Willingham, Characterization of the antigen (CAK1) recognized by monoclonal antibody K1 present on ovarian cancers and normal mesothelium, Cancer Res. 52 (1) (1992) 181–186.

[4] X. Liu, A. Chan, C.H. Tai, T. Andresson, I Pastan, Multiple proteases are involved in mesothelin shedding by cancer cells, Commun. Biol. 3 (1) (2020) 728.

[5] M. Ho, M. Onda, Q.C. Wang, R. Hassan, I. Pastan, M.O. Lively, Mesothelin is shed from tumor cells, Cancer Epidemiol. Biomarkers Prev. 15 (9) (2006) 1751.

[6] E. Sharon, J. Zhang, K. Hollevoet, S.M. Steinberg, I. Pastan, M. Onda, et al., Serum mesothelin and megakaryocyte potentiating factor in pancreatic and biliary cancers, Clin. Chem. Lab Med. 50 (4) (2012) 721–725.

[7] R. Hassan, A. Thomas, C. Alewine, D.T. Le, E.M. Jaffee, I Pastan, Mesothelin Immunotherapy for Cancer: ready for Prime Time? J. Clin. Oncol. 34 (34) (2016) 4171–4179.

[8] S. Inaguma, Z. Wang, J. Lasota, M. Onda, P. Czapiewski, R. Langfort, et al., Comprehensive immunohistochemical study of mesothelin (MSLN) using different monoclonal antibodies 5B2 and MN-1 in 1562 tumors with evaluation of its prognostic value in malignant pleural mesothelioma, Oncotarget 8 (16) (2017) 26744–26754.

[9] S. Weidemann, P. Gagelmann, N. Gorbokon, M. Lennartz, A. Menz, A.M. Luebke, et al., Mesothelin Expression in Human Tumors: a Tissue Microarray Study on 12,679 Tumors, Biomedicines 9 (4) (2021).

[10] R. Hassan, A.T. Remaley, M.L. Sampson, J. Zhang, D.D. Cox, J. Pingpank, et al., Detection and quantitation of serum mesothelin, a tumor marker for patients with mesothelioma and ovarian cancer, Clin. Cancer Res. 12 (2) (2006) 447–453.

[11] Y. Yu, B.M. Ryan, A. Thomas, B. Morrow, J. Zhang, Z. Kang, et al., Elevated Serum Megakaryocyte Potentiating Factor as a Predictor of Poor Survival in Patients with Mesothelioma and Primary Lung Cancer, J. Appl. Lab Med. 3 (2) (2018) 166–177.

[12] L. Cao, Y. Yu, A. Thomas, J. Zhang, M. Onda, P. Meltzer, et al., Megakaryocyte Potentiating Factor as a Predictive Biomarker for Therapies Against Malignant Mesothelioma, JCO Precision Oncol. 2018 (2018).

[13] R. Hassan, Z.G. Laszik, M. Lerner, M. Raffeld, R. Postier, D Brackett, Mesothelin is overexpressed in pancreaticobiliary adenocarcinomas but not in normal pancreas and chronic pancreatitis, Am. J. Clin. Pathol. 124 (6) (2005) 838–845.

[14] C. Alewine, M. Ahmad, C.J. Peer, Z.I. Hu, M.J. Lee, A. Yuno, et al., Phase I/II Study of the Mesothelin-targeted Immunotoxin LMB-100 with nab-paclitaxel for Patients with Advanced Pancreatic Adenocarcinoma, Clin. Cancer Res. (2019).

[15] J. Zhang, S. Qiu, Y. Zhang, M. Merino, P. Fetsch, I. Avital, et al., Loss of mesothelin expression by mesothelioma cells grown in vitro determines sensitivity to anti-mesothelin immunotoxin SS1P, Anticancer Res. 32 (12) (2012) 5151–5158.

[16] L.R. Avula, M. Rudloff, S. El-Behaedi, D. Arons, R. Albalawy, X. Chen, et al., Mesothelin enhances tumor vascularity in newly forming pancreatic peritoneal metastases, Mol. Cancer Res. (2019).

[17] H.L. Beyer, R.D. Geschwindt, C.L. Glover, L. Tran, I. Hellstrom, K.E. Hellstrom, et al., MESOMARK: a potential test for malignant pleural mesothelioma, Clin. Chem. 53 (4) (2007) 666–672.

[18] Y. Zhang, L. Xiang, R. Hassan, I Pastan, Immunotoxin and Taxol synergy results from a decrease in shed mesothelin levels in the extracellular space of tumors, in: Proceedings of the National Academy of Sciences of the United States of America 104, 2007, pp. 17099–17104.

[19] J.A. Gubbels, J. Belisle, M. Onda, C. Rancourt, M. Migneault, M. Ho, et al., Mesothelin-MUC16 binding is a high affinity, N-glycan dependent interaction that facilitates peritoneal metastasis of ovarian tumors, Mol. Cancer 5 (1) (2006) 50.

[20] Y. Zhang, I Pastan, High shed antigen levels within tumors: an additional barrier to immunoconjugate therapy, Clin. Cancer Res. 14 (24) (2008) 7981–7986.

[21] P. Awuah, T.K. Bera, M. Folivi, O. Chertov, I Pastan, Reduced Shedding of Surface Mesothelin Improves Efficacy of Mesothelin-Targeting Recombinant Immunotoxins, Mol. Cancer Ther. 15 (7) (2016) 1648–1655.

[22] Y. Zhang, O. Chertov, J. Zhang, R. Hassan, I Pastan, Cytotoxic activity of immunotoxin SS1P is modulated by TACE-dependent mesothelin shedding, Cancer Res. 71 (17) (2011) 5915–5922.

[23] K.A. Lofgren, S. Sreekumar, E.C. Jenkins Jr., K.J. Ernzen, P.A Kenny, Anti-tumor efficacy of an MMAE-conjugated antibody targeting cell surface TACE/ADAM17-cleaved Amphiregulin in breast cancer, Antib. Ther. 4 (4) (2021) 252–261.

[24] S.K. Shukla, V. Gunda, J. Abrego, D. Haridas, A. Mishra, J. Souchek, et al., MUC16-mediated activation of mTOR and c-Myc reprograms pancreatic cancer metabolism, Oncotarget 6 (22) (2015) 19118–19131.

[25] E. Tomas-Bort, M. Kieler, S. Sharma, J.B. Candido, D. Loessner, 3D approaches to model the tumor microenvironment of pancreatic cancer, Theranostics 10 (11) (2020) 5074–5089.